

Chapter 6

Application of Remote Sensing

Glaciers and glacial lakes are generally located in remote areas, where access is through tough and difficult terrain. The study of glaciers and glacial lakes, as well as carrying out glacial lake outburst flood (GLOF) inventories and field investigations using conventional methods, requires, extensive time and resources together with undergoing hardship in the field. Creating inventories and monitoring of the glaciers, glacial lakes, and extent of GLOF impact downstream can be done quickly and correctly using satellite images and aerial photographs. Use of these images and photographs for the evaluation of physical conditions of the area provides greater accuracy. The multi-stage approach using remotely sensed data and field investigation increases the ability and accuracy of the work. Visual and digital image analysis techniques integrated with techniques of geographic information systems (GIS) are very useful for the study of glaciers, glacial lakes, and GLOFs.

At first the inventory and evaluation of the glaciers, glacial lakes, and GLOFs were carried out based on topographic maps. The topographic maps of the higher terrain, which houses glaciers and glacial lakes, are not as reliable as those of hills and lowland areas. As a complementary data and tool, various remote sensing techniques and satellite images were used.

Remote sensing is the science and art of acquiring information (spectral, spatial, temporal) about material objects, areas, or phenomena through the analysis of data acquired by a device from measurements made at a distance, without coming into physical contact with the objects, area, or phenomena under investigation.

Remote sensing technology makes use of the wide range of the electro-magnetic spectrum (EMS). Most of the commercially available remote-sensing data are acquired in the visible, infrared, and microwave wavelength portion of the EMS. For the present study, the data acquired within the visible and infrared wavelength ranges were used.

There are different types of commercial satellite data available. Digital data sets of the Land Observation Satellite (LANDSAT)-5 Thematic Mapper (TM) and Indian Remote Sensing Satellite Series 1D (IRS1D) Linear Imaging and Self Scanning Sensor (LISS)3 were used mostly for the present study. Some data sets of Système Probatoire Pour l'Observation de la Terre (SPOT) Multi-Spectral (XS) and SPOT Panchromatic (PAN) were also used. The list of the images and aerial photographs relevant to the present study are given in Chapter 4.

A scene of a LANDSAT TM image gives the synoptic view of an area of 185 km by 170 km of the Earth's surface sensed by the American LANDSAT satellite from an altitude of 705 km. There are seven spectral bands of electromagnetic spectrum in LANDSAT TM data, ranging from the blue to far infrared wave length (Figure 6.1). The individual bands are 0.45–0.52, 0.53–0.60, 0.62–0.69, 0.78–0.90, 1.57–1.78, and 2.10–2.35 μm with the spatial resolution of 30m in the visible, near infrared and middle infrared bands, and 10.45–11.66 μm in the far infrared band with 120m resolution. Some of the potential applications of different spectral bands of LANDSAT TM are given in Table 6.1. The TM sensors greatly facilitate the multi-temporal data availability (repeated coverage of 16 days) for studying the temporal changes of glaciers, lakes, and other features.

Band number	Band range (μm)	Potential applications
1	0.45–0.52	Coastal water mapping; soil/vegetation differentiation; deciduous/coniferous differentiation (sensitive to chlorophyll concentration) etc
2	0.52–0.62	Green reflectance by healthy vegetation etc
3	0.63–0.69	Chlorophyll absorption for plant species' differentiation
4	0.78–0.90	Biomass surveys; water body delineation
5	1.55–1.75	Vegetation moisture measurement; snow/cloud differentiation; snow/ice quality study
6	10.4–12.5	Plant heat stress management; other thermal mapping; soil moisture discrimination
7	2.08–2.35	Hydro-thermal mapping; discrimination of mineral and rock types; snow/cloud differentiation; snow/ice quality study

The SPOT series of French satellites and recent series of IRS satellites have more advantages for the study of glaciers, glacial lakes, and GLOFs due to their stereo data acquisition capacity ($\pm 26^\circ$ off-nadir viewing capability of the system) and higher spatial resolutions of 6 (IRS1C/IRSID PAN data) to 10m (SPOT PAN data).

LISS3 sensors on board IRS1C/D satellites provide multi-spectral data collected in four bands of VNIR (visible and the near infrared) and SWIR (short wave infrared) regions (Tables 6.2 and 6.3). LISS3 images cover an area of 124 by 141 km for the VNIR bands (B2, B3, B4) and 133 by 148 km for the SWIR band (B5) sensed from an altitude of 817 km (IRS1C) to 780 km (IRS1D) with repetitive coverage of 25 days. The spatial resolution of VNIR bands is 24m and that of SWIR is 71m.

The spatial resolution of LISS3 of the IRS satellite series and XS of the SPOT satellite series are greater than that of LANDSAT TM. With a greater number of spectral bands and spatial resolution of 30 by 30m close to the former two data types, cloud free LANDSAT TM data are equally good for the inventory and evaluation of glaciers, glacial lakes, and GLOFs in the medium scale (1:100,000 to 1:25,000). One can compare the amount of detail in different images covering the same area of Lunana region in Figures 6.4 and 6.5.

When electro-magnetic energy is incident on any given Earth surface feature, three fundamental energy interactions with the feature are possible. Various fractions of energy incident on the element are reflected, absorbed, and/or transmitted. All components of incident, reflected, absorbed, and/or transmitted energy are a function of the wavelength. The proportions of energy reflected, absorbed, and transmitted vary for different Earth features, depending on their material types and conditions. These differences permit us to distinguish different features on an image. Thus, two features may be distinguishable in one spectral range and may be very different on another wavelength band. Within the visible portion of the spectrum, these spectral variations result in the visual effect called **colour**. For example, blue objects reflect highly in the blue portion of the spectrum, likewise green reflects highly in the 'green' spectral region, and so on. Thus, the eye uses spectral variations in the magnitude of reflected energy to discriminate between various objects.

Satellite data are digital records of the spectral reflectance of the Earth's surface features. These digital values of spectral reflectance are used for image processing and image interpretations. A graph of the spectral reflectance of an object as a function of wavelength is called a spectral reflectance curve. The

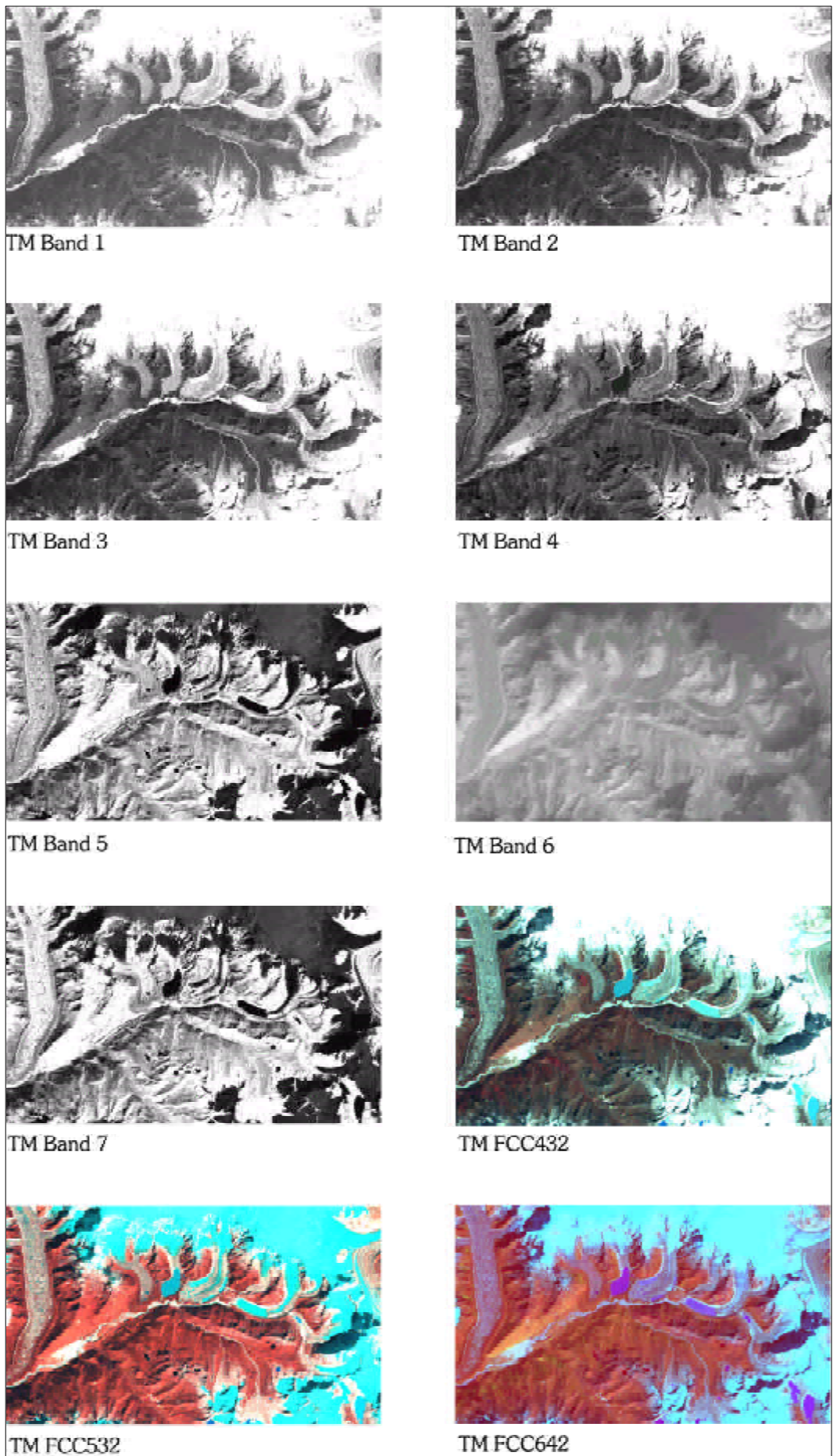


Figure 6.1: Subset of LANDSAT 5 TM image (Path 138 Row 041) of 4 November 1998 of Lunana region in the Pho Chu Basin of Bhutan

Satellite system Optical sensor system (Launch dates)	LANDSAT 4/5 MSS (1982 LANDSAT-4) (1985 LANDSAT -5)	LANDSAT 4/5 TM (1982 LANDSAT-4) (1984 LANDSAT-5) (1999 LANDSAT -7)	SPOT XS (1986 SPOT-1) (1990 SPOT-2) (1993 SPOT-3) (1999 SPOT-4)	IRS-1C LISS-III (1995 IRS-1C) (1997 IRS-1D)
Sensor altitude	LANDSAT 1,2,3 = 900 km LANDSAT 4, 5 = 705 km	705 km	832 km	817 km
Spatial resolution	80m	30m	20m	24m
Temporal resolution (revisit cycle in days)	16	16	20 (nadir)	24 (nadir)
Radiometric resolution (bits per pixel)	6-bit (scaled to 7 or 8-bit during ground processing)	8-bit	8-bit	7-bit
Swath width	185 km scene area = 185*170	185 km scene area = 185*170	60 km	141 km 124*141 133*148
Off-nadir viewing (side-look) capability for PAN mode for stereo image data acquisition ($\pm 26^\circ$ off-nadir viewing)			SPOT PAN (10 m resolution) 0.51–0.73 μm 3 days revisit capability	IRS-1C PAN (6 m resolution) (70 km swath width) 0.50–0.70 μm (6-bit) 3 days revisit capability
Spectral resolution (number of bands)	4	7	3	4

Satellites system Optical sensor system	LANDSAT 4/5 MSS	LANDSAT 4/5 TM	SPOT XS	IRS-1C/1D LISS-III
Blue		0.45–0.52 μm (B1)		
Green	0.50–0.60 μm (Ch1 or B4)	0.53–0.61 μm (B2)	0.50–0.59 μm (XS1)	0.52–0.59 μm (B2)
Red	0.60–0.70 μm (Ch2 or B5)	0.62–0.69 μm (B3)	0.62–0.68 μm (XS3)	0.62–0.68 μm (B3)
NIR	0.70–0.80 μm (Ch3 or B6)	0.78–0.90 μm (B4)	0.78–0.88 μm (XS3)	0.77–0.86 μm (B4)
NIR	0.80–1.10 μm (Ch4 or B7)			
IIR		1.57–1.78 μm (B5)		1.55–1.75 μm (B5)
IIR		2.10–2.35 μm (B7)		
IIR (MIR)				
ThIR		10.45–11.66 μm (B6)		
FIR				

configuration of spectral reflectance curves provides insight into the characteristics of an object and has a strong influence on the choice of wavelength region(s) in which remote-sensing data are acquired for a particular application.

Figure 6.2 (over page) shows the typical spectral reflectance curves for three basic types of Earth feature: green vegetation, soil, and water. The lines in this figure represent average reflectance curves compiled by measuring large sample features. It should be noted how distinctive the curves are for each feature. In general, the configuration of these curves is an indicator of the type and condition of the features to

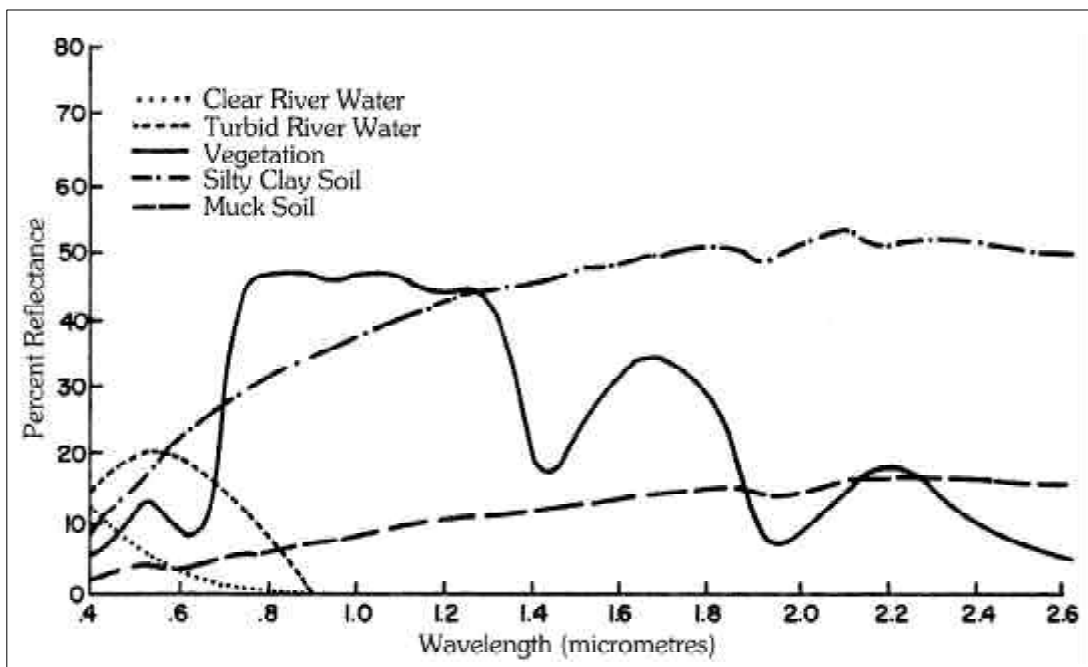


Figure 6.2: Typical spectral reflectance curves for vegetation, soil, and water(after Swain and Davis 1979)

which they apply. Although the reflectance of individual features may vary considerably above and below the average, these curves demonstrate some fundamental points concerning spectral reflectance.

Spectral reflectance curves for vegetation almost always manifest the 'peak-and-valley' configuration (Figure 6.2). Valleys in the different parts of the spectral reflectance curve are the result of the absorption of energy due to plants, leaves, pigments, and chlorophyll content at 0.45 and 0.67 μm wavelength bands and water content at 1.4, 1.9, and 2.7 μm wavelength bands. In near infrared spectrum wavelength bands ranging from about 0.7–1.3 μm , plants reflect 40–50% of energy incident upon them. The reflectance is due to plant leaf structure and is highly variable among plant species, which permits discrimination between species. Different plant species reflect differently in different portions of wavelength.

The soil curve in Figure 6.2 shows considerably less peak-and-valley variation in reflectance. This is because the factors that influence soil reflectance act over less specific spectral bands. Some of the factors affecting soil reflectance are moisture content, soil texture (proportion of sand, silt, and clay), surface roughness, presence of iron oxide, and organic matter content. These factors are complex, variable, and inter-related. For example, the presence of moisture in soil will decrease its reflectance. As with vegetation, this effect is greatest in the water absorption bands at about 1.4, 1.9, and 2.7 μm (clay soils also have hydroxyl absorption bands at about 1.4 and 2.2 μm). Soil moisture content is strongly related to soil texture; coarse and sandy soils are usually well drained, resulting in low moisture content and relatively high reflectance; poorly drained and fine-textured soils will generally have lower reflectance. In the absence of water, however, the soil may exhibit the reverse tendency, that is, coarse-textured soils may appear darker than fine-textured soils. Thus, the reflectance properties of soil are consistent only within a particular range of conditions. Two other factors that reduce soil reflectance are surface roughness and organic matter content. Soil reflectance normally decreases when surface roughness and organic matter content increases. The presence of iron oxide in soil also significantly decreases reflectance, at least in the visible wavelengths. In any case, it is essential that the analyst be familiar with the existing conditions.

When considering the spectral reflectance of water, probably the most distinctive characteristic is the energy absorption at near infrared wavelengths. Water absorbs energy in these wavelengths, whether considering water features per se (such as lakes and streams) or water contained in vegetation or soil. Locating and delineating water bodies with remote-sensing data are carried out easily in near infrared wavelengths because of this absorption property. However, various conditions of water bodies manifest themselves primarily in visible wavelengths. The energy/matter interactions at these wavelengths are very complex and depend on a number of inter-related factors. For example, the reflectance from a water body can stem from an interaction with the water surface (specular reflection), with material suspended in the water, or with the bottom of the water body. Even in deep water where bottom effects are negligible, the

reflectance properties of a water body are not only a function of the water per se but also of the material in the water.

Clear water absorbs relatively little energy with wavelengths of less than about $0.6 \mu\text{m}$. High transmittance typifies these wavelengths with a maximum in the blue-green portion of the spectrum. However, as the turbidity of water changes (because of the presence of organic or inorganic materials), transmittance, and therefore reflectance, changes dramatically. This is true in the case of water bodies in the same geographic area. Spectral reflectance increases as the turbidity of water increases. Likewise, the reflectance of water depends on the concentration of chlorophyll. Increases in chlorophyll concentration tend to decrease water reflectance in blue wavelengths and increase it in green wavelengths. Many important water characteristics, such as dissolved oxygen concentration, pH, and salt concentration, cannot be observed directly through changes in water reflectance. However, such parameters sometimes correlate with observed reflectance. In short, there are many complex inter-relationships between the spectral reflectance of water and its particular characteristics. One must use appropriate reference data to correctly interpret reflectance measurements made over water.

Snow and ice are the frozen state of water. Early work with satellite data indicated that snow and ice could not be reliably mapped because of the similarity in spectral response between snow and clouds due to limitations in the then available data set. Today satellite remote sensing systems' data are available in more spectral bands (e.g. LANDSAT TM in seven bands). It is now possible to differentiate snow and cloud easily in the middle infrared portion of the spectrum, particularly in the $1.55\text{--}1.75$ and $2.10\text{--}2.35 \mu\text{m}$ wavelength bands (bands 5 and 7 of LANDSAT TM). As shown in Figure 6.3, in these wavelengths, the clouds have a very high reflectance and appear white on the image, while the snow has a very low reflectance and appears black on the image. In the visible, near infrared, and thermal infrared bands, spectral discrimination between snow and clouds is not possible, while in the middle infrared it is. The reflectance of snow is generally very high in the visible portions and decreases throughout the reflective infrared portions of the spectrum. The reflectance of old snow and ice is always lower than that of fresh snow and clean/fresh glacier in all the visible and reflective infrared portions of the spectrum. Compared to clean glacier and snow (fresh as well as old), debris covered glacier and very old/dirty snow have much lower reflectance in the visible portions of the spectrum and higher in the middle infrared portions of spectrum.

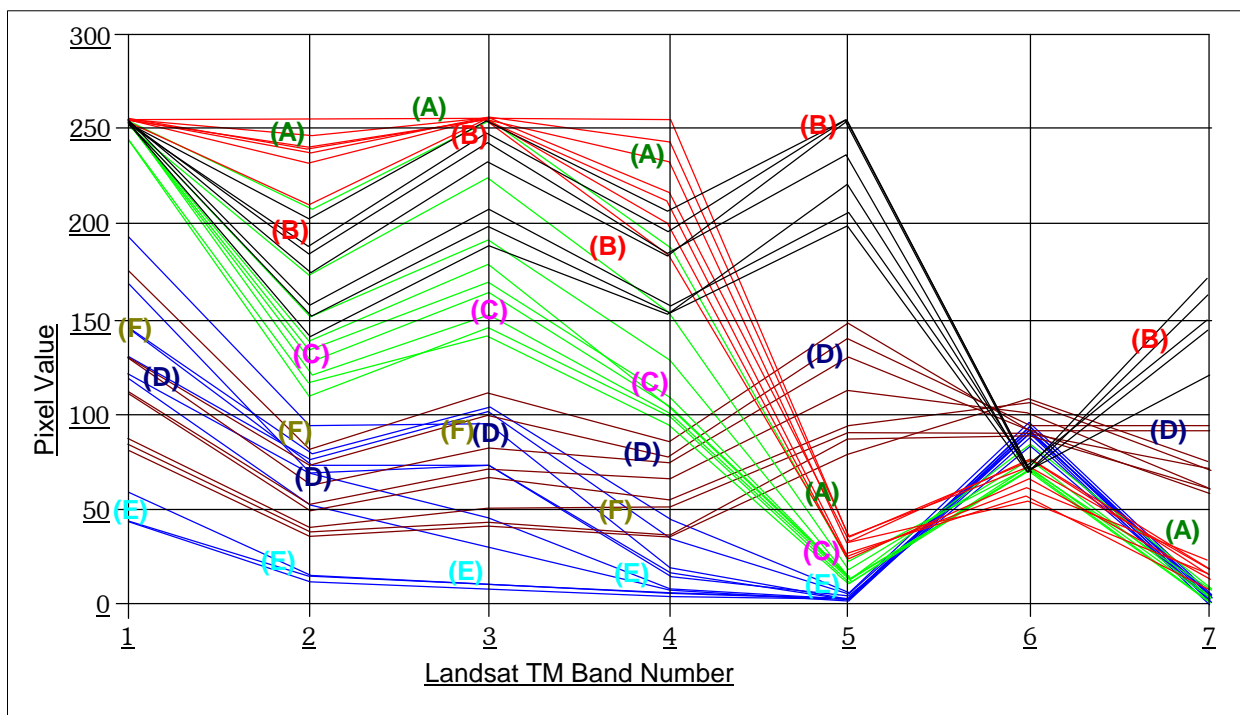


Figure 6.3: Spectral reflectance characteristics of snow/ice, clean glaciers, debris covered glaciers, clouds, and water bodies. Reflectance in terms of pixel value based on LANDSAT TM seven-band data set of the Pho Chu area of Bhutan. Red lines—clean glaciers and fresh snow (A); black lines—clouds (B); green lines—old snow/glaciers (C); maroon lines—debris covered glacier (D); blue lines—clean/melted (E) and silty and/or partly frozen water (lake/river) (F)

To identify the individual glaciers and glacial lakes, different image enhancement techniques are useful. However, complemented by the visual interpretation method (visual pattern recognition), with the knowledge and experience of the terrain conditions, glacier and glacial lake inventories and monitoring can be done. With different spectral band combinations in false colour composite (FCC) and in individual spectral bands, glaciers and glacial lakes can be identified and studied using the knowledge of image interpretation keys: colour, tone, texture, pattern, association, shape, shadow etc. Combinations of different bands can be used to prepare FCC. Different colour composite images highlight different land-cover features.

Figure 6.4 shows colour composite images R7G4B3 (red to band 7, green to band 4, blue to band 3) of a LANDSAT 4 TM image of 4 November 1998 of Lunana area in the Pho Chu Basin and R4G3B2 of an IRS1D LISS3 of 12 December 1999 of the same area. In the colour composite images of Figure 6.4 and the panchromatic images of Figure 6.5 one can identify different types of land cover, glaciers, glacial lakes, and GLOF events such as: (A) Raphstreng Tsho Glacial Lake; (B) debris covered tongue of Thorthormi Glacier with some frozen lakes; (C) Lugge Tsho Glacial Lake showing the breached area at the moraine; (D) Drukchang Glacier tongue with frozen lake; (E) debris covered Bechung Glacier tongue with lake; (F) debris covered Tsonglu Glacier; (G) the Pho Cho River showing the effect of debris flow from Lugge Tsho Lake on 4 October 1994; (H) clean glaciers and fresh snow area; and (I) erosion lakes (showing in black)

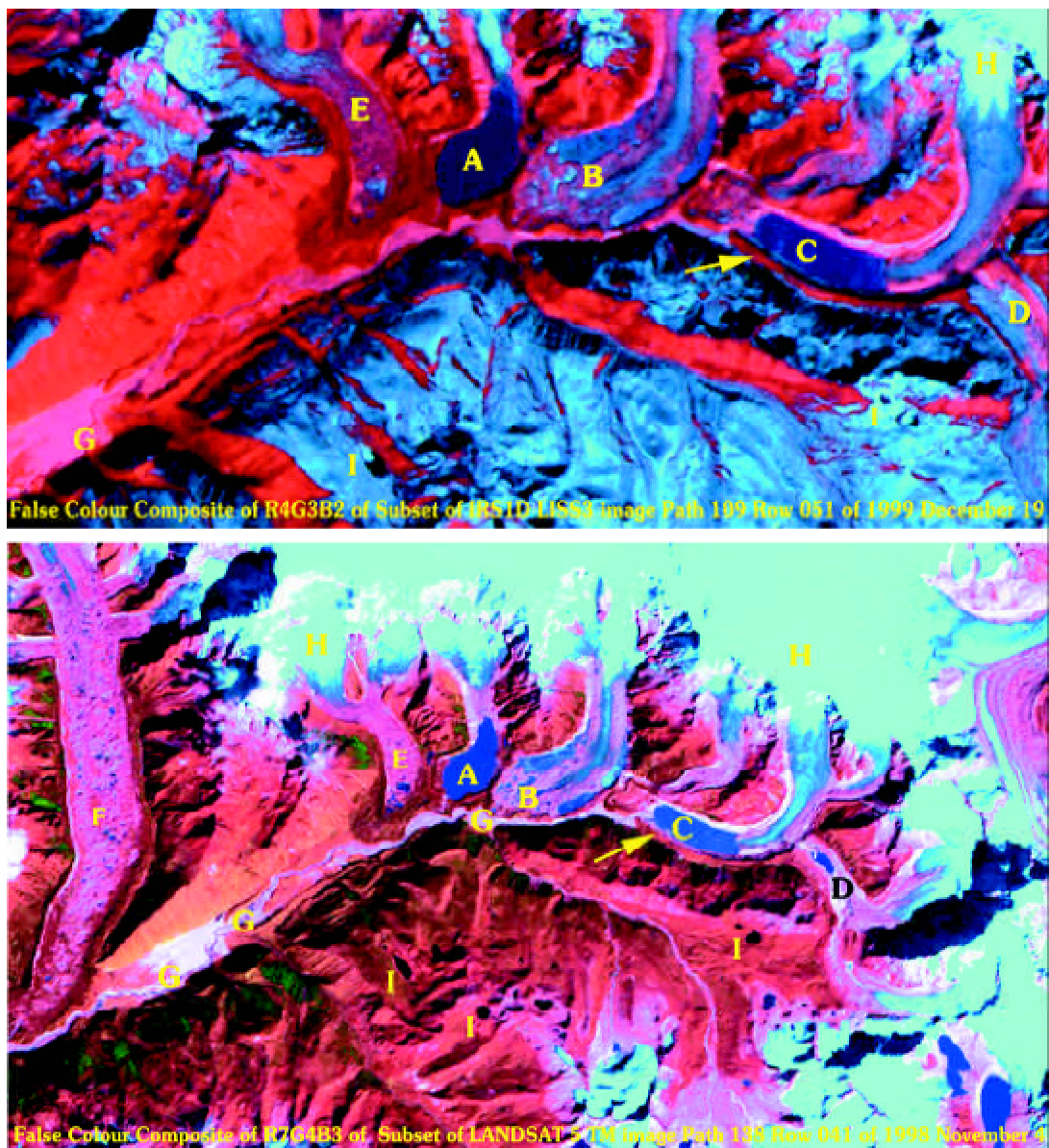


Figure 6.4: Colour composite of IRS1D LISS3 (12 December 1999) showing the Lunana region in the Pho Chu Basin of Bhutan: (A) Raphstreng Tsho Glacial Lake, the upper part of the lake near the glacier tongue is frozen; (B) debris covered tongue of Thorthormi Glacier with some frozen lakes; (C) Lugge Tsho Glacial Lake showing the breached area at the moraine; (D) Drukchang Glacier tongue with frozen lake; (E) debris covered Bechung Glacier tongue with lake; (F) debris covered Tsonglu Glacier; (G) the Pho Cho River showing the effect of debris flow from Lugge Tsho Lake on 4 October 1994; (H) clean glaciers and fresh snow area; and (I) erosion lakes (showing in black)

the moraine; (D) Drukchang glacier tongue with frozen lake; (E) debris covered Bechung glacier tongue with lake; (F) debris covered Tsonglu Glacier; (G) Pho Cho showing the effect of debris flow from Lugge Tsho Lake on 4 October 1994; and (H) clean glacier and fresh snow area. Colours in the colour composite images and tones in the individual band images are the outcome of the reflectance values. Glaciers appear white (in individual bands and colour composite) to light blue (in colour composite) colour of variable sizes, with linear and regular shape having fine to medium texture, whereas, in the thermal band, they appear grey to black. The distinct linear and dendritic pattern associated with slopes and valley floors of the high mountains covered with seasonal snow can be distinguished in the glaciers in the mountains.

The lake water in colour composite images ranges in appearance from light blue to blue to black. In the case of frozen lakes, it appears white. Sizes are generally small, having circular, semi-circular, or elongated shapes with very fine texture and are generally associated with glaciers in the case of high lying areas, or rivers in the case of low lying areas. In general, erosion lakes and some cirque lakes are not necessarily associated with glaciers or rivers at present. The debris flow path along the drainage channel gives a white to light grey and bright tone.

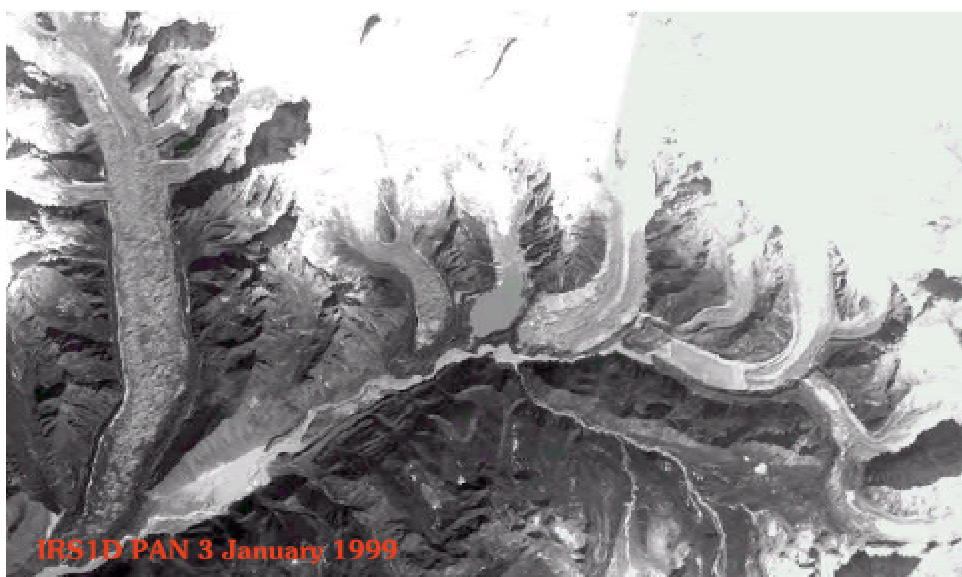
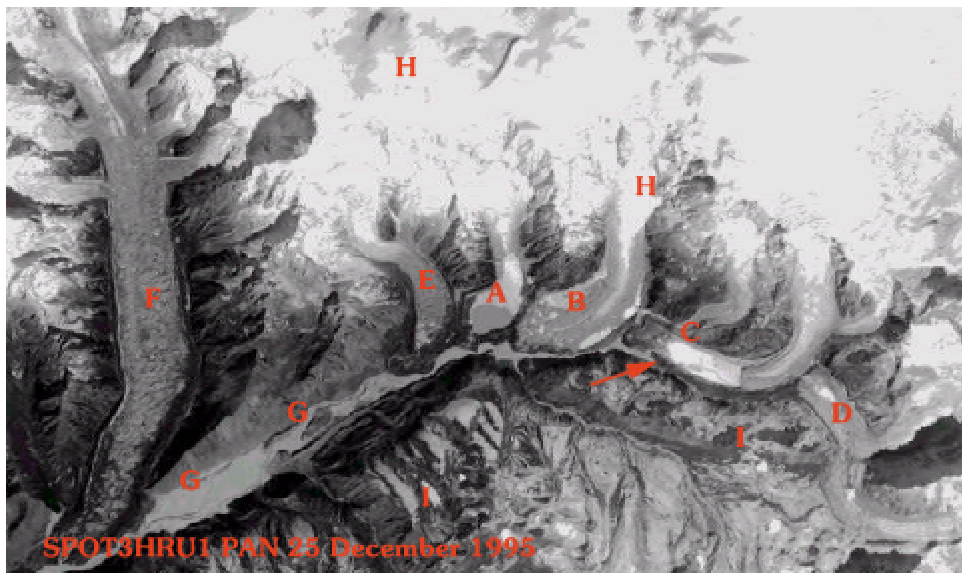


Figure 6.5: Panchromatic image of Raphstreng Lake area in the Pho Chu Basin of Bhutan: (A) Raphstreng Tsho Glacial Lake, the upper part of the lake near the glacier tongue is frozen; (B) debris covered tongue of Thorthormi Glacier with some frozen lakes; (C) Lugge Tsho Glacial Lake showing the breached area at the moraine; (D) Drukchang Glacier tongue with frozen lake; (E) debris covered Bechung Glacier tongue with lake; (F) debris covered Tsonglu Glacier; (G) the Pho Cho River showing the effect of debris flow from Lugge Tsho Lake on 4 October 1994; (H) clean glaciers and fresh snow area; and (I) erosion lakes (showing in white)

For glacier and glacial lake identification from satellite images, the images should be with least snow cover and cloud free. Least snow cover in the Himalayas occurs generally in the summer season (May–September). But during this season, monsoon clouds will block the views. If snow precipitation is late in the year, winter images are also suitable except for the problem of long relief shadows in the high mountain regions. For the present study, most of the images are of the winter season under conditions of least seasonal snow cover and cloud free.

Knowledge of the physical characteristics of the glaciers, lakes, and their associated features is always necessary for the interpretation of the images. For example, the end moraine damming the lake may range from a regular curved shape to a semi-circular crescent shape. The frozen lake and glacier ice field may have the same reflectance, but the frozen lake always has a level surface and is generally situated in the ablation areas of glaciers or at the toe of the glacier tongue, and there is greater possibility of association with drainage features downstream.

The technique of digital image analysis facilitates image enhancement and spectral classification of the ground features and, hence, greatly helps in the study of glaciers and lakes. Monitoring of the lakes and glaciers can be done visually as well as digitally. In both the visual interpretation and digital feature extraction techniques, the analyst's experience and adequate field knowledge are necessary. The satellite images have to be geometrically rectified based on the appropriate geo-reference system and cell sizes. The same geo-reference system is required for the integration and analysis of the remote sensing satellite data in the GIS database. The image resolutions and geo-reference system should be the same for better results. Figure 6.6 shows an example of Raphstreng Lake area on two different dates. The images are projected in the same geo-reference system and resampled into the same size. The two-date images show the change in physical condition and the process related to the glacial lake; they indicate the fast growth of Raphstreng Glacial Lake at the tongue of Raphstreng Glacier and the enlargement of supraglacial lakes at the tongue of Thorthormi Glacier. The supra-glacial ponds at the tongue of Thorthormi glacier are enlarged and merged in the new date image to form a bigger pond (lake). This is, again, an indication of the fast development of a glacial lake at the tongue of Thorthormi Glacier.



Figure 6.6: Raphstreng Lake and glacier tongue of Thorthormi Glacier on 25 December 1994 (left side) and on 3 January 1999 (right side)

The lakes that have already burst in the past can be identified from the disturbed damming materials and the drainage characteristics associated with the lake. Figure 6.7 shows the situation before and after the breaching on 4 October 1994 of Lugge Tsho Glacier at the tongue of Lugge Glacier dammed by ice cored moraine. An ice-core moraine dam usually has a hummock dissected end moraine, with smaller ponds in some cases. The lateral moraine ridges are generally of a smooth, narrow, linear appearance and are easily identifiable on the images. Figure 6.8 shows the breaching of Lugge Tsho Glacial Lake at the area of contact of lateral moraine and end moraine. Lugge Tsho Glacial Lake, which burst on 7 October 1994, carrying lots of debris along the Pho Chu, is visible on the images. The channel path along which glacial lake outburst flooding has occurred shows distinct light tone widths along the drainage channel and banks due to bank erosion and deposition at different places along the river. The loose materials transported and deposited along the streams have higher spectral reflectance compared to their surroundings and old stable river channels, which appear relatively lighter and brighter.

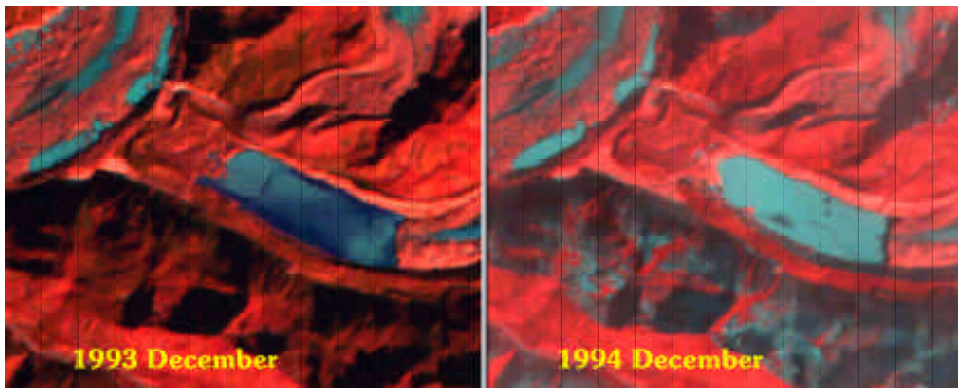


Figure 6.7: False colour composite R5G3B2 of LANDSAT TM showing Luge Thso Lake before and after breaching on 7 October 1994



Figure 6.8: IRS1C PAN data of 3 January 1999 draped on the DEM showing the breached area of Luge Tsho Lake on 7 October 1994

Coarse spatial resolution images have limitations when distinguishing smaller lakes and small stream paths. However, such small objects will show up in the coarse spatial resolution images averaged with reflectance values of their surrounding objects.

The technique of integrating remote sensing data with GIS does help a lot with identification and monitoring of lakes and glaciers. The DEM of an area generated either using stereo satellite images, aerial photographs, or digitisation of topographic map data can play a big role in deciding the rules for discrimination of features and land cover types in GIS techniques and for better perspective viewing and presentations. DEM itself can be used to create various data sets of the area (e.g. slope, aspect). For example, even though glacial lakes are covered by snow, the lake surfaces are flat, and glaciers, snow, and ice create slope angles. In this case, decision rules for integrated analysis in GIS can be assigned, that is, if the slope is not too pronounced and the texture smooth, then such areas are recognised as frozen glacial lakes. DEM generated from satellite images, aerial photographs, or topographic maps should be compatible with and of reliable quality to other data sets. The satellite images or orthophotos can be draped over the DEM for interpretation or presentation. Figures 6.9 and 6.10 show some examples of the use of DEM draped by satellite images.

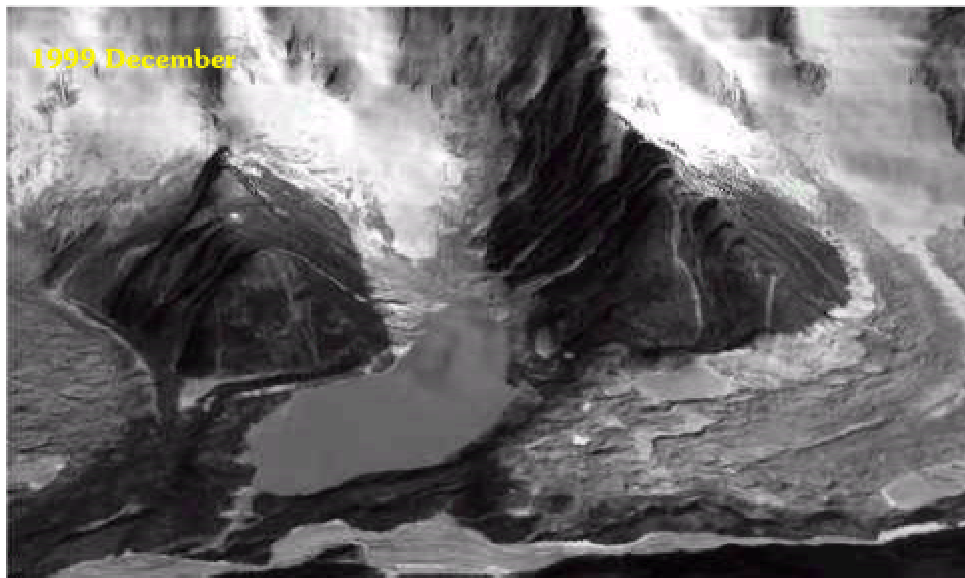
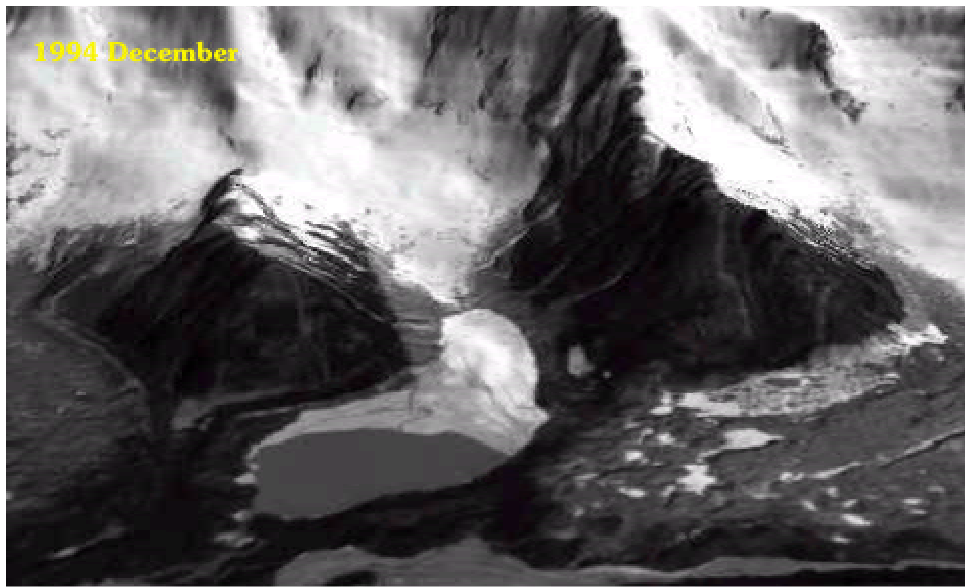


Figure 6.9: Raphstreng Lake and glacier tongue of Thorthormi Glacier on 25 December 1994 (SPOT PAN) and on 3 January 1999 (IRS 1C PAN). Both the images are draped over the DEM generated from the topographic map on a scale of 1:50,000

Based on different criteria, actively retreating glaciers and potentially dangerous lakes can be determined using the developed spatial and attribute database complemented by multi-temporal remote-sensing data sets. Once the activity of glaciers and the potentially dangerous status of lakes are determined, the use of medium- to large-scale aerial photographs provides the best tool for detailed geomorphic studies and other evaluation. The photograph image characteristics, shape, shadow, tone, colour, texture, pattern, and relation to surrounding objects were used for aerial photo interpretation. Geomorphic features and processes of the area are very distinctive in their appearance on aerial photographs. Physical parameters of glaciers, glacial lakes, and associated moraines can easily be estimated by stereoscopic viewing. Aerial photographs for Bhutan are not available for the present study.

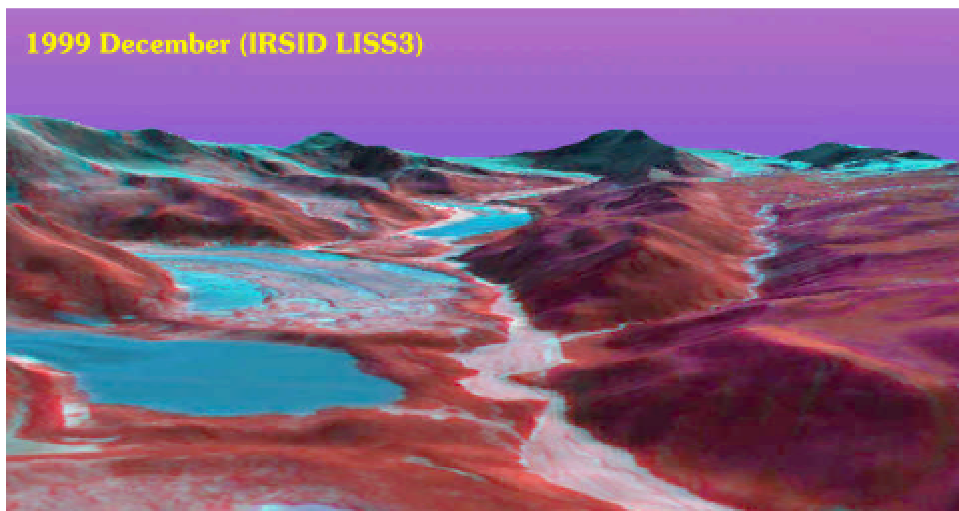
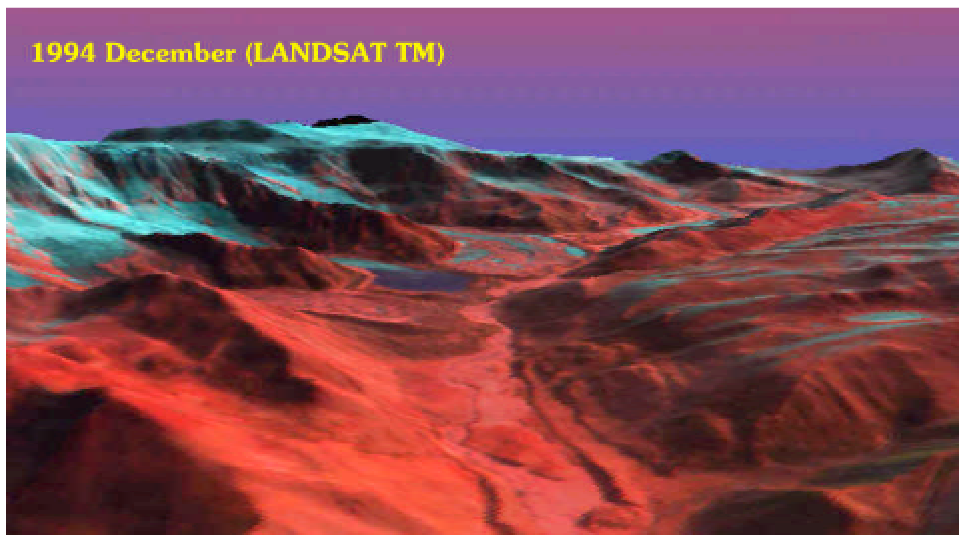
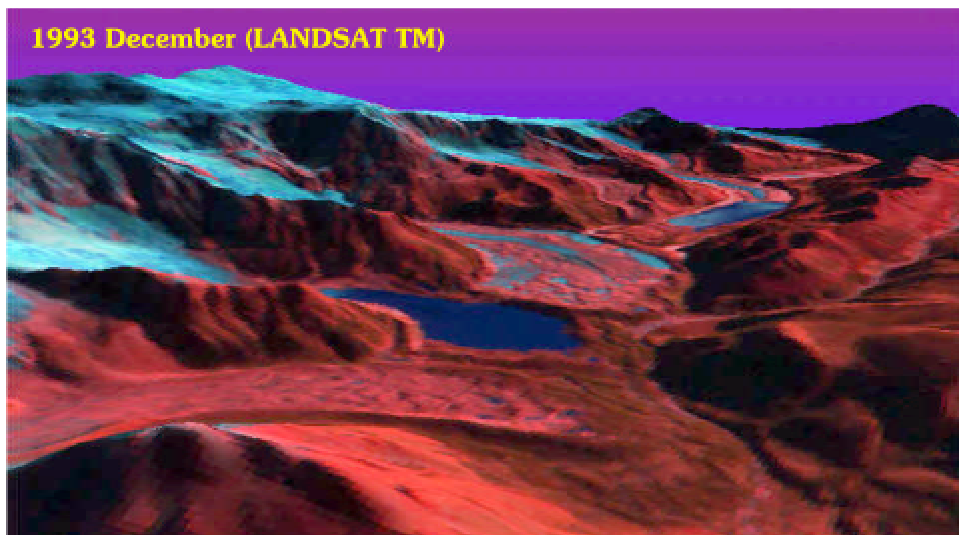


Figure 6.10: Three-dimensional perspective view of Raphstreng Tsho and Lugge Tsho area in the Pho Chu Sub-basin of Bhutan overlaid on a DEM generated from the topographic map on a scale of 1:50,000. 50° angle of field of view, -12° pitch, 90° azimuth, 1,434m above ground level of viewer position situated at $x = 2762127$ and $y = 1147216$. The effect of Lugge Tsho GLOF is clearly visible in the 1999 image